

# On the Efimov Effect in Higher Partial Waves

K. Helfrich and H.-W. Hammer

*Helmholtz-Institut für Strahlen- und Kernphysik (Theorie)*  
*and Bethe Center for Theoretical Physics,*  
*Universität Bonn, 53115 Bonn, Germany*  
(Dated: November 20, 2018)

## Abstract

Using the framework of effective field theory, we present a detailed study of the Efimov effect in higher partial waves for systems of two identical particles and a third distinguishable particle. Depending on the total angular momentum  $L$ , the two identical particles must be bosons or fermions. We derive analytical expressions for the elastic and inelastic atom-dimer scattering cross sections as well as the atom-dimer relaxation rate at the dimer breakup threshold. For the experimentally most relevant case of P-waves, we numerically calculate the atom-dimer scattering cross sections and relaxation rates as a function of the scattering length, three-body parameter, and mass ratio for energies below breakup threshold.

PACS numbers: 34.50.-s, 67.85.Pq

## I. INTRODUCTION

The last few years saw an enormous progress in the field of Efimov physics, theoretically as well as experimentally [1]. Already in 1970, Efimov predicted the existence of universal three-body bound states with a geometric spectrum for identical bosons at infinite scattering length  $a$  [2]

$$B_t^{(n)} = \left(e^{-2\pi/s_0}\right)^{n-n_*} \hbar^2 \kappa_*^2 / m, \quad (1)$$

where  $m$  is the mass of the particles,  $s_0 \approx 1.00624$  is a transcendental number, and  $\kappa_*$  is the binding wave number of the state labelled  $n_*$ . This leads to an accumulation point at  $E = 0$  and a discrete scale invariance with a scaling factor of  $e^{\pi/s_0} \approx 22.7$ . Away from unitarity, there is only a finite number of bound states. As the inverse scattering length is varied from negative to positive values, an Efimov state appears at the three-particle scattering threshold at  $a = a_-$ , crosses the unitary limit at  $1/a = 0$  with the energy given in Eq. (1), and vanishes at  $a = a_*$  through the atom-dimer threshold. Whenever an Efimov trimer hits one of these thresholds, recombination rates get enhanced [3–5].

Measuring this enhancement, the Efimov effect has by now been observed in bosonic isotopes of cesium [6, 7], potassium [8], and lithium [9, 10]. The case of fermionic lithium with three different hyperfine states is similar to the bosonic case in many aspects. Because of the three different pair scattering lengths involved, however, the phenomenology is much richer. After the indirect observation via resonant enhancement of the recombination rates [11, 12], the direct association of Efimov trimers was also achieved [13, 14].

Mixed systems also allow for the appearance of the Efimov effect as long as at least two of the scattering lengths are resonant. This is most easily realised with two different atomic species, one of which has to be bosonic for the S-wave case. If the bosonic species is much heavier than the other one, the scaling factor can become considerably smaller and thus more favorable for the experimental investigation [15]. This case has been considered in detail in [16]. The first experimental measurement of the Efimov effect in a bosonic rubidium-potassium mixture was reported in [17].

However, if the heavy species in a heteronuclear mixture is fermionic, the Efimov effect is only present in a P-wave channel and only if the masses differ by at least a factor of 13.61 [15]. This behaviour can be generalized to higher partial waves. The parameters  $s_L$  determining the scaling factor for total angular momentum  $L$  can be estimated by [15]

$$s_L^2 \approx s_0^2 - L(L + 1), \quad (2)$$

where  $s_0$  characterizes the corresponding scaling factor for zero angular momentum.  $s_L^2 \geq 0$  must be fulfilled for the occurrence of the Efimov effect (also see more detailed discussion in section II). The necessary mass ratios for the P-wave case ( $L = 1$ ) could be realised for example with  ${}^6\text{Li}$ - ${}^{87}\text{Sr}$ ,  ${}^{6/7}\text{Li}$ - ${}^{137}\text{Ba}$ ,  ${}^{6/7}\text{Li}$ - ${}^{167}\text{Er}$ , or  ${}^{6/7}\text{Li}$ - ${}^{171/173}\text{Yb}$ . Higher partial waves would only become accessible if hydrogen or helium atoms can be used. Dimer-dimer scattering in heteronuclear mixtures showing a P-wave Efimov effect was investigated in [18].

The main focus of this paper is also on such mixtures, prepared as atom-dimer systems. We study in detail how the Efimov effect in higher partial waves affects observables such as atom-dimer scattering and atom-dimer relaxation. We briefly introduce our effective field theory framework and derive analytical expressions for the elastic and inelastic atom-dimer scattering cross sections at the dimer breakup threshold. For the P-wave case, we numerically calculate the atom-dimer scattering cross sections and relaxation rates as a function of the

scattering length, three-body parameter, and mass ratio below dimer breakup threshold. Finally, some quantities for systems without Efimov effect are also computed.

## II. FRAMEWORK

In the following, we investigate various heteronuclear atomic systems in detail and closely follow the formalism and conventions of Ref. [16]. For convenience, we set  $\hbar = 1$  but restore the dimensions for final results. We consider systems consisting of two different atomic species, where the occurring trimers, Efimov or non-Efimov, are built of one atom of type 1 and two atoms of type 2. The unlike particles have a resonant S-wave interaction which can be tuned using a Feshbach resonance whereas the interaction between identical particles can be neglected. The corresponding Lagrangian is given by [16]

$$\begin{aligned} \mathcal{L} = & \Psi_1^\dagger \left( i\partial_t + \frac{\nabla^2}{2m_1} \right) \Psi_1 + \Psi_2^\dagger \left( i\partial_t + \frac{\nabla^2}{2m_2} \right) \Psi_2 \\ & + g_2 d^\dagger d - g_2 \left( d^\dagger \Psi_1 \Psi_2 + \Psi_1^\dagger \Psi_2^\dagger d \right) - \frac{g_3}{4} d^\dagger d \Psi_2^\dagger \Psi_2 + \dots, \end{aligned} \quad (3)$$

where  $m_{1/2}$  denotes the mass of particles of species 1/2,  $g_{2/3}$  are the bare two-body and three-body coupling constants, and  $d$  is an auxiliary field for a dimer consisting of particle species 1 and 2. The first two terms in Eq. (3) are the kinetic terms for species 1 and 2, while the third term is the kinetic term for the non-dynamical auxiliary dimer field which mediates the interactions between the particles of species 1 and 2. It becomes dynamical through the coupling to particle loops. The fourth and fifth terms generate the S-wave contact interactions between particles of species 1 and 2 and a three-body interaction between one particle of species 1 and two particles of species 2.<sup>1</sup> The ellipses stand for higher-order terms containing more fields and/or derivatives. As in Ref. [16], we denote the ratio of the masses of particle species 1 and 2 by  $\delta \equiv m_1/m_2$ . In this study, however, we explicitly focus on higher partial waves with total angular momentum  $L > 0$ .

Because of symmetry reasons, the Efimov effect can only occur in even angular momentum channels if the two like particles are bosons and in odd angular momentum channels if they are fermions [19]. In the following, we will refer to the first case as *bosonic* and the second case as *fermionic* for simplicity. The nature of the third particle is not relevant for our purpose. For inverse mass ratios  $\delta^{-1}$  larger than a critical ratio  $\delta_{c,L}^{-1}$ , Efimov physics can be observed [15]. At  $\delta_{c,L}^{-1}$  and beyond, the angular momentum barrier is overcome by the attractive interaction between unlike particles (cf. Eq. (2)). The light particle can be thought of as an exchange particle between the two heavy atoms. In this case, the “fall to the center” phenomenon typical for the Efimov effect can happen. A (hybrid) Born-Oppenheimer description has been used in the limit of a very light particle of species 1 [18, 20]. In the case of  $L = 1$ , the mass ratio must satisfy  $\delta^{-1} \gtrsim 13.61 = \delta_{c,1}^{-1}$  [15, 21]. The D-wave Efimov effect starts at  $\delta^{-1} \gtrsim 38.63 = \delta_{c,2}^{-1}$  [15, 22] and its observation would always be obscured by the already present S-wave effect. Consequently, the fermionic P-wave case is the only relevant one in cold atom experiments besides the S-wave bosonic case. The mass ratios  $\delta^{-1}$  for some possible mixtures showing the P-wave Efimov effect are given in Table I.

---

<sup>1</sup> To this order, the coefficient of the dimer kinetic term is not independent of the interaction between particles 1 and 2 and can be chosen as  $g_2$  for convenience.

	<sup>87</sup> Sr	<sup>137</sup> Ba	<sup>167</sup> Er	<sup>171</sup> Yb	<sup>173</sup> Yb
<sup>6</sup> Li	14.5	22.8	27.8	28.5	28.8
<sup>7</sup> Li	-	19.6	23.9	24.4	24.7

TABLE I. Mass ratios  $\delta^{-1}$  for possible experimental mixtures showing the P-wave Efimov effect.

It is straightforward to derive Feynman rules and to obtain the full dimer propagator from the Lagrangian in Eq. (3) (for more details, see Refs. [16, 23]). In the three-body system, we obtain an integral equation for the off-shell atom-dimer scattering amplitude  $\mathcal{A}_L(p, k; E)$  known as the STM equation [24]. The amplitude depends on the relative momenta of the atom and the dimer in the initial state,  $k$ , and in the final state,  $p$ , as well as on the total energy  $E$ . All three-body observables can be obtained from this amplitude evaluated in appropriate kinematics. Projecting on total angular momentum  $L$ , the equation becomes

$$\begin{aligned} \mathcal{A}_L(p, k; E) = & (\pm 1) \frac{2\pi m_1}{a\mu^2} \frac{1}{pk} (-1)^L Q_L \left( \frac{p^2 + k^2 - 2\mu E}{2pk\mu/m_1} \right) \\ & + (\pm 1) \frac{m_1}{\pi\mu} \int_0^{\Lambda_c} dq \frac{q}{p} (-1)^L Q_L \left( \frac{p^2 + q^2 - 2\mu E}{2pq\mu/m_1} \right) \\ & \times \frac{\mathcal{A}_L(q, k; E)}{-1/a + \sqrt{-2\mu(E - q^2/(2\mu_{AD}))}}, \end{aligned} \quad (4)$$

where the prefactor  $+1$  corresponds to the atoms of species 2 being bosons and  $-1$  to fermions, respectively. Moreover,  $\mu = m_1 m_2 / (m_1 + m_2)$  is the reduced mass of two unlike atoms,  $\mu_{AD} = m_2 (m_1 + m_2) / (m_1 + 2m_2)$  is the reduced mass of an atom and a dimer,

$$Q_L(z) = \frac{1}{2} \int_{-1}^1 dx \frac{P_L(x)}{z - x} \quad (5)$$

is a Legendre function of the second kind, and  $P_L(x)$  is a Legendre polynomial. The log-periodic dependence of the three-body interaction  $g_3$  on the cutoff has been used to absorb the complex three-body parameter into the momentum cutoff  $\Lambda_c$  in Eq. (4) [5]. The integration in Eq. (4) is along a straight line in the complex plane from zero to  $\Lambda_c$ . The physical values of the amplitude  $\mathcal{A}$  are obtained by evaluating Eq. (4) once more for real  $p = k$  after the solution along the complex contour has been obtained. The absolute value of the cutoff  $\Lambda_c$  is proportional to the binding momentum of the deepest Efimov state, whereas the complex phase determines the width of the Efimov trimers,  $\Lambda_c \propto e^{i\eta_*/s_L} \kappa_*$ . Physically, the parameter  $\eta_*$  takes into account the effects of deeply-bound dimers which provide decay channels for the Efimov trimers [5]. For S-wave Feshbach resonances,  $\eta_*$  is typically of the order 0.1. In the limit of small  $\eta_*/s_L$ , the width of Efimov trimers is given by

$$\Gamma_t \approx \frac{4\eta_*}{s_L} \left( B_t + \frac{\hbar^2}{2\mu a^2} \right), \quad (6)$$

where  $B_t$  is the trimer energy (cf. Eq. (259) in Ref. [23]). Thus for small  $\eta_*/s_L$ , the width becomes small. Without knowing  $\eta_*$ , a quantitative prediction is not possible, but we generally expect lifetimes comparable to the S-wave case if  $s_L$  is of order one.

In the channels without the Efimov effect (odd angular momenta for bosons, even angular momenta for fermions, or for  $\delta^{-1} < \delta_{c,L}^{-1}$ ), the absolute value of the momentum cutoff  $\Lambda_c$  can

be taken to infinity. The three-body interaction in Eq. (3) is higher order in these channels and all observables are in leading order determined by the scattering length alone.

### III. SCALING FACTOR AND RESONANCE POSITIONS

If more than one Efimov resonance feature can be measured in an experiment, the scaling factor  $\exp(\pi/s_L)$  can be deduced. The quantity  $s_L$  can be computed analytically by considering the large momentum behaviour of Eq. (4) [25–27]. In this limit the energies and inverse scattering lengths can be neglected compared to the momenta  $p$  and  $q$ , the inhomogeneous term as well as purely polynomial terms in the integral kernel are suppressed, and the momentum integration can be extended to infinity. This leads to the equation

$$\tilde{\mathcal{A}}_L(p) = (\pm 1)(-1)^L \frac{m_1}{\pi\mu} \sqrt{\frac{\mu_{AD}}{\mu}} \int_0^\infty \frac{dq}{q} P_L\left(\frac{p^2 + q^2}{2pq\mu/m_1}\right) Q_0\left(\frac{p^2 + q^2}{2pq\mu/m_1}\right) \tilde{\mathcal{A}}_L(q), \quad (7)$$

where we have defined  $\tilde{\mathcal{A}}_L(p) \equiv p\mathcal{A}_L(p, k; E)$ . Since the equation is scale invariant, it has power law solutions. If the Efimov effect is present, the exponent is complex:  $\tilde{\mathcal{A}}_L(p) \propto p^{\pm is_L}$ . Identifying the right hand side of Eq. (7) as a Mellin transform, we then obtain a transcendental equation for  $s_L$ :

$$1 = \pm \frac{(-1)^L}{\sin(2\phi)} \sum_{k=0}^{k_{max}} \frac{(2L-2k)!}{(L-k)!k!} \frac{(-1)^k}{2^{2L-2k}(\sin\phi)^{L-2k}} \times \sum_{m=0}^{L-2k} \frac{1}{m!(L-2k-m)!} \frac{2}{is_L + 2m - L + 2k} \frac{\sin[(is_L + 2m - L + 2k)\phi]}{\cos[(is_L + 2m - L + 2k)\frac{\pi}{2}]}, \quad (8)$$

where we defined

$$\phi = \arcsin \frac{1}{\delta + 1}, \quad (9)$$

and

$$k_{max} = \begin{cases} L/2 & \text{if } L \text{ is even} \\ (L-1)/2 & \text{if } L \text{ is odd} \end{cases}. \quad (10)$$

In the case  $L = 1$ , Eq. (8) reduces to

$$1 = \frac{1}{2\sin^2\phi\cos\phi} \left[ \frac{1}{is_1 - 1} \frac{\sin[(is_1 - 1)\phi]}{\cos[(is_1 - 1)\pi/2]} + \frac{1}{is_1 + 1} \frac{\sin[(is_1 + 1)\phi]}{\cos[(is_1 + 1)\pi/2]} \right]. \quad (11)$$

The corresponding equation for  $L = 2$  is given by

$$1 = \frac{3}{8\sin^3\phi\cos\phi} \left[ \frac{1}{is_2 - 2} \frac{\sin[(is_2 - 2)\phi]}{\cos[(is_2 - 2)\pi/2]} + \frac{1}{is_2 + 2} \frac{\sin[(is_2 + 2)\phi]}{\cos[(is_2 + 2)\pi/2]} + \frac{2 - 4/3\sin^2\phi}{is_2} \frac{\sin[is_2\phi]}{\cos[is_2\pi/2]} \right]. \quad (12)$$

An equivalent equation for general  $L$  using hypergeometric functions was derived by Nielsen and coworkers [19]. The results of Eqs. (11) and (12) coincide with the ones obtained by making use of Eq. (117) in [19]. The critical mass ratios  $\delta_{c,L}$  are obtained by observing when  $s_L$  tends to zero. We find  $\delta_{c,1}^{-1} = 13.61$  and  $\delta_{c,2}^{-1} = 38.63$  in agreement with previous

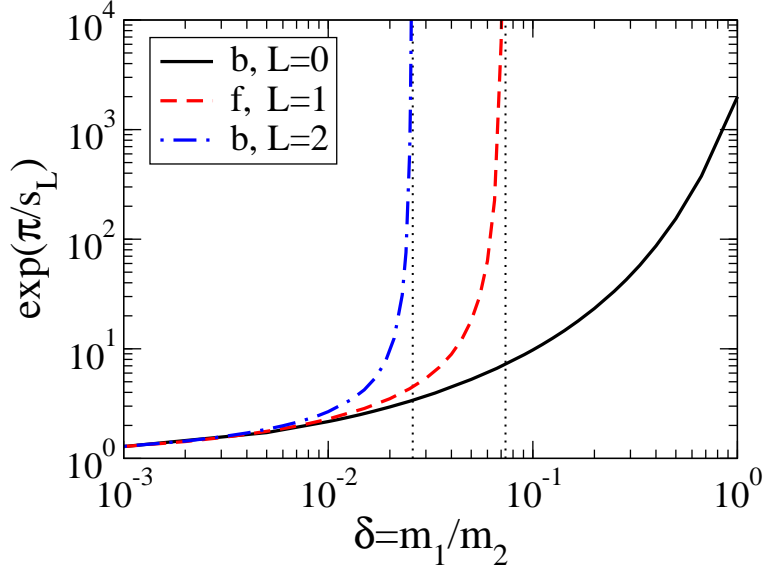


FIG. 1. Scaling factors  $\exp(\pi/s_L)$  for bosons (b) and fermions (f) as a function of the mass ratio  $\delta = m_1/m_2$  for  $L = 0, 1, 2$ , respectively. The vertical dotted lines indicate the critical mass ratios  $\delta_{c,1}$  and  $\delta_{c,2}$  for the Efimov effect with  $L = 1, 2$ .

determinations [21, 22]. The resulting scaling factors  $\exp(\pi/s_L)$  are shown in Fig. 1 as a function of the mass ratio  $\delta = m_1/m_2$ . The critical mass ratios  $\delta_{c,1}$  and  $\delta_{c,2}$  for  $L = 1, 2$  can be read off from the positions where the scaling factor diverges (indicated by the vertical dotted lines). For  $L \rightarrow \infty$ , the critical mass ratio approaches zero. For  $\delta \rightarrow 0$ , all scaling factors approach unity corresponding to the limit  $s_L \rightarrow \infty$ .

Another important observable is the ratio  $a_*/|a_-|$  that compares the values of the scattering length  $a_*$  and  $a_-$  at which Efimov trimers cross the atom-dimer and three-particle thresholds, respectively. This ratio can be measured experimentally if at least one resonance feature is seen for negative scattering length and one in the atom-dimer system. The calculated ratios for  $L = 1$  are shown in Fig. 2 for following one Efimov state and for comparing neighbouring states as a function of the mass ratio  $\delta = m_1/m_2$ .

#### IV. ANALYTICAL RESULTS FOR ATOM-DIMER SCATTERING

The scattering of atoms and dimers can be directly related to the STM equation (4) with equal incoming and outgoing momenta. The scattering amplitude is given by

$$f_L(k) = \frac{k^{2L}}{k^{2L+1} \cot \delta_{AD,L}(k) - ik^{2L+1}} = \frac{\mu_{AD}}{2\pi} \mathcal{A}_L(k, k; E), \quad (13)$$

where the energy  $E$  and center-of-mass momentum  $k$  are related by  $E = k^2/(2\mu_{AD}) - B_d$ . The dimers are built of two unlike particles and their binding energy is given by  $B_d = 1/(2\mu a^2)$ . The dimer breakup threshold at  $E = 0$  corresponds to  $k = \sqrt{\mu_{AD}/\mu}/a \equiv k_D$ . It is useful to define an energy dependent *scattering length*,

$$\tilde{a}_{AD,L}(k) = \frac{-1}{k^{2L+1} \cot \delta_{AD,L}(k)}. \quad (14)$$

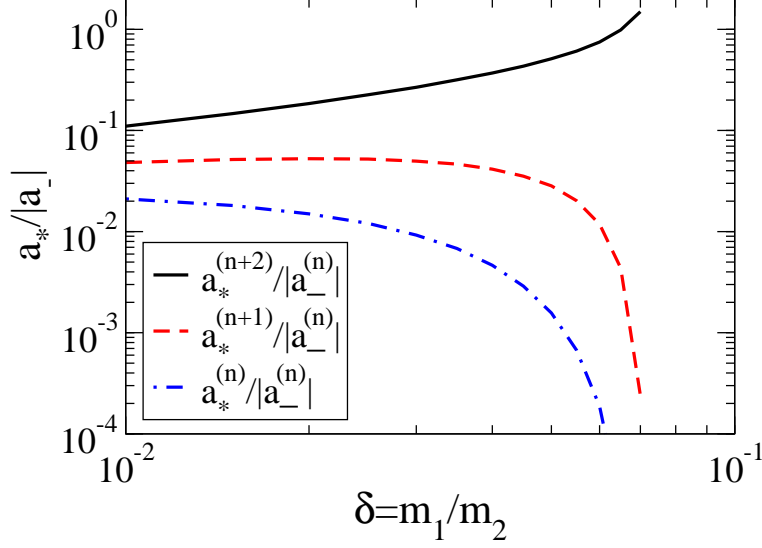


FIG. 2. The ratio  $a_*/|a_-|$  for following one Efimov state and for comparing neighbouring states as a function of the mass ratio  $\delta = m_1/m_2$  in the case  $L = 1$ .

Note that this quantity does not have the dimension of a length for  $L > 0$ . We can now calculate the elastic atom-dimer scattering cross section in the  $L$ th partial wave

$$\sigma_{AD,L}^{(\text{el})}(k) = (2L + 1)4\pi |f_L(k)|^2. \quad (15)$$

The total cross section can be obtained with the help of the optical theorem

$$\sigma_{AD,L}^{(\text{tot})}(k) = (2L + 1)\frac{4\pi}{k}\text{Im}f_L(k), \quad (16)$$

and the inelastic cross section  $\sigma_{AD,L}^{(\text{inel})}(k)$  by subtracting Eqs. (16) and (15).

At  $E = 0$ , it is also possible to deduce these quantities analytically using the methods of Section IV of Ref. [16]. If the Efimov effect is present, the S-matrix element for elastic atom-dimer scattering can be written as

$$S_L = -e^{2i\sigma_L} \cosh(\pi s_L + i s_L \log(a/a_{0*}) - \eta_*) / \cosh(\pi s_L - i s_L \log(a/a_{0*}) + \eta_*), \quad (17)$$

where  $\sigma_L$  is a real number and  $a_{0*}$  determines the position of the minima in the three-body recombination rate for positive scattering length and in the elastic atom-dimer cross section. Hence, the elastic cross section can be expressed as

$$\begin{aligned} \sigma_{AD,L}^{(\text{el})}(E = 0) &= (2L + 1)\frac{\pi}{k_D^2} |S_L - 1|^2 \\ &= (2L + 1)4\pi a^2 \frac{\delta(\delta + 2)}{(\delta + 1)^2} \frac{\sinh^2(\pi s_L) \{ \sinh^2(\eta_*) + \sin^2[s_L \log(a/a_{0*})] \}}{\sinh^2(\pi s_L + \eta_*) + \cos^2[s_L \log(a/a_{0*})]}, \end{aligned} \quad (18)$$

where  $k_D a = (\delta + 1)/\sqrt{\delta(\delta + 2)}$  was used. The inelastic cross section is given by

$$\begin{aligned} \sigma_{AD,L}^{(\text{inel})}(E = 0) &= (2L + 1)\frac{\pi}{k_D^2} (1 - |S_L|^2) \\ &= (2L + 1)\pi a^2 \frac{\delta(\delta + 2)}{(\delta + 1)^2} \frac{\sinh(2\pi s_L) \sinh(2\eta_*)}{\sinh^2(\pi s_L + \eta_*) + \cos^2[s_L \log(a/a_{0*})]}. \end{aligned} \quad (19)$$

Atom-dimer relaxation is the process where an atom and a shallow dimer collide and an energetic deep dimer and atom are ejected. It is one of the main loss processes in mixtures of atoms and dimers. The atom-dimer relaxation rate constant  $\beta$  is defined by the rate equation

$$\frac{d}{dt}n_D = \frac{d}{dt}n_A = -\beta n_D n_A, \quad (20)$$

where  $n_{A/D}$  denotes the number densities of atoms and dimers, respectively. The relaxation rate is directly related to the inelastic scattering cross section,

$$\beta_L(E) = \frac{k}{\mu_{AD}} \sigma_{AD,L}^{(\text{inel})}(E). \quad (21)$$

At  $E = 0$ , we therefore obtain

$$\beta_L(E = 0) = (2L + 1)\pi \frac{\sqrt{\delta(\delta + 2)}^3}{(\delta + 1)^2} \frac{\sinh(2\pi s_L) \sinh(2\eta_*)}{\sinh^2(\pi s_L + \eta_*) + \cos^2[s_L \log(a/a_{0*})]} \frac{\hbar a}{m_1}. \quad (22)$$

We note that our analytical results for the inelastic atom-dimer rate at zero energy are in agreement with the general scaling law derived by D’Incao and Esry [28]. At the atom-dimer threshold,  $E = -B_d$ , only the S-wave contribution survives. This case was studied in detail in Ref. [16]. For all other angular momenta  $L > 0$ , the atom-dimer scattering amplitude, Eq. (13), vanishes for  $k \rightarrow 0$ .

Another important process in cold atom experiments is three-body recombination. This process can happen in a mixture if not all atoms of species 1 are bound in dimers. The atom of species 1 and an atom of species 2 form a dimer, shallow or deep, and another atom of species 2 balances energy and momentum. Typically, all three atoms are lost if this process occurs in a trap. For angular momenta  $L > 0$ , however, the three-body recombination rate vanishes at  $E = 0$ .

In the following, we present numerical results for the atom-dimer observables discussed above focussing on the experimentally most relevant case  $L = 1$ .

## V. NUMERICAL RESULTS

### A. Atom-dimer observables without Efimov effect

In this subsection, we only consider the case  $\eta_* = 0$  which corresponds to no deeply-bound dimers. As a consequence, the inelastic cross section vanishes below the dimer breakup threshold. In the P-wave channel, there is no Efimov effect for bosons. The total (=elastic) atom-dimer scattering cross section for  $E = 0$  (at dimer breakup) is shown as the solid line in Fig. 3. Note that for increasing  $\delta^{-1}$ , the cross section does not tend monotonically to zero but rather oscillates with diminishing amplitude. This oscillation is not due to the crossing of bound three-body states with the atom-dimer threshold as three-body bound states are not present in this system (see below for the fermionic case). Using Eq. (15), the elastic cross section at threshold can be written as

$$\sigma_{AD,L}^{(\text{el})}(k_D) = (2L + 1)4\pi a^2 \frac{(1 + 2\delta^{-1})}{(1 + \delta^{-1})^2} \sin^2 \delta_{AD,L}(k_D). \quad (23)$$

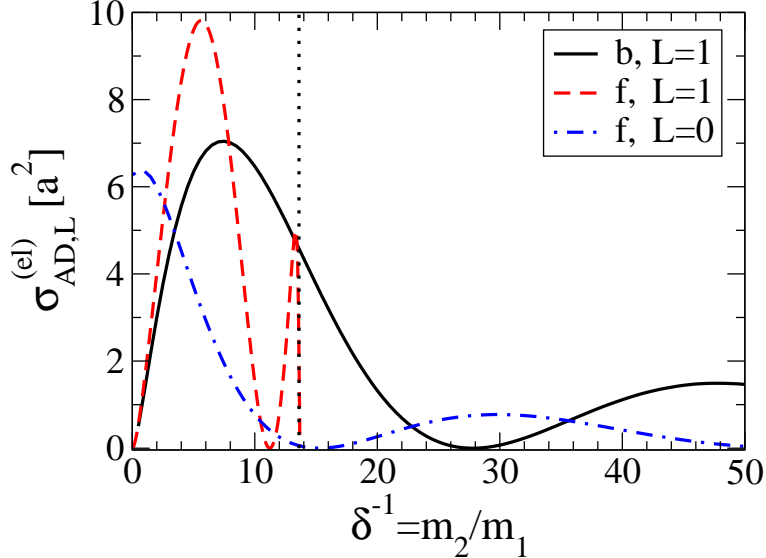


FIG. 3. The elastic atom-dimer scattering cross sections for bosons (b) and fermions (f) in the P-wave channel and for fermions in the S-wave channel at  $E = 0$  as a function of the mass ratio  $\delta^{-1}$ . The vertical dotted line indicates the critical mass ratio for fermions in the P-wave channel,  $\delta_{c,1}^{-1} = 13.61$ .

The observed oscillation then implies a monotonic dependence of the elastic phase shift at threshold on  $\delta^{-1}$  [29] with  $\delta_{AD,L}(k_D) = 0$  for  $\delta^{-1} = 0$ . For decreasing energy, the amplitude of the cross section gets larger and the peaks move to larger mass ratios  $\delta^{-1}$ .

A similar behavior is observed for fermions in the S-wave channel. The atom-dimer scattering length can be determined according to the formula  $a_{AD,0} = -\mathcal{A}_0(0, 0; -B_d)\mu_{AD}/(2\pi)$ . This reproduces the results for the mass dependence found by Petrov [21] that were confirmed in Refs. [30, 31]. The corresponding total cross section is shown in Fig. 3 as dash-dotted line. Again, the oscillation is not due to bound states and Eq. (23) implies a monotonic dependence of the threshold phase shift on  $\delta^{-1}$ . However, in this case  $\delta_{AD,L}(k_D)$  approaches a value slightly below  $\pi/2$  for  $\delta^{-1} = 0$ . As in the case of bosons with  $L = 1$ , we find that the amplitude of the cross section gets larger for decreasing energy and the peaks move to larger mass ratios  $\delta^{-1}$ .

For fermions in the P-wave channel, the Efimov effect only comes into play for mass ratios  $\delta^{-1} \gtrsim 13.61$ . For the region without the Efimov effect, many observables have already been calculated [29, 32–36]. Kartavtsev and Malykh found one three-body bound state for the range  $8.17260 < \delta^{-1} < 12.91743$  and two three-body bound states for  $12.91743 < \delta^{-1} < 13.6069657$  [29]. They call these states *universal*, as their binding energies only depend on the dimer binding energy, or equivalently, the scattering length. The occurrence of these states was recently confirmed by Endo et al. [36]. They also demonstrated the divergence of the atom-dimer scattering length at the mass ratios where the universal trimer states appear and how similar behaviour occurs for higher angular momenta. We have confirmed these results. Kartavtsev and Malykh also found that close to the critical mass ratio, the energies of the universal states follow a square-root dependence [29],  $E - E_c \propto \sqrt{\delta_{c,1}^{-1} - \delta^{-1}}$ . An investigation of the behavior of Efimov states for  $\delta^{-1}$  slightly above  $\delta_{c,1}^{-1}$  would be interesting.

The behavior of the energies must be non-analytic in  $\delta^{-1} - \delta_{c,1}^{-1}$ , since Efimov states can be shifted to any desired energy by adjusting the three-body parameter. However, such a study is beyond the scope of the present investigation as our numerical calculations converge only slowly close to the critical mass ratio.

In Ref. [29], atom-dimer elastic scattering at the dimer breakup threshold was also calculated. We show this process as the dashed line in Fig. 3 in comparison to the results for bosons with  $L = 1$  and for fermions with  $L = 0$ . In order to elucidate the physics of the

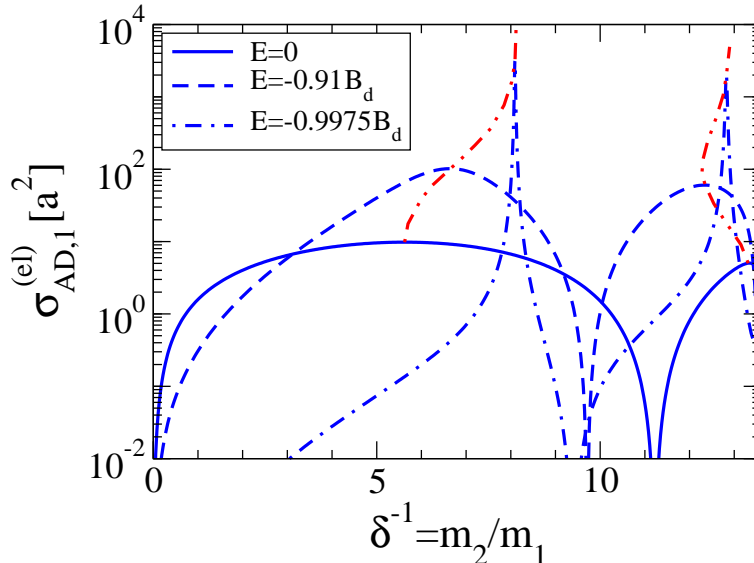


FIG. 4. The elastic cross section  $\sigma_{AD,1}^{(el)}$  in units of  $a^2$  versus the mass ratio  $\delta^{-1}$  at the energies  $E = 0, -0.91B_d$ , and  $-0.9975B_d$  (solid, dashed, dash-dotted lines). The dash-double-dotted lines indicate the position of the two peaks for varying energy.

two peaks in the elastic cross section, we show our results for  $\sigma_{AD,1}^{(el)}$  in Fig. 4 as a function of  $\delta^{-1}$  for three energies,  $E = 0, -0.91B_d$ , and  $-0.9975B_d$ , i.e., at and below the dimer breakup threshold. The dash-double-dotted lines show how the peak positions move with varying energy. While the first peak moves monotonically to larger values of  $\delta^{-1}$  as the energy is decreased, the second peak shows a more complicated behavior. Initially, it moves to smaller values and reaches a minimum  $\delta_{\min}^{-1} \approx 12.3$  for  $E/B_d \approx -0.938$ , before it moves back to larger values of  $\delta^{-1}$  as the atom-dimer threshold is approached. Our results demonstrate that the two-peak structure is indeed due to the presence of the two universal three-body bound states. The positions of the two peaks move from  $\delta^{-1} = 5.63$  and  $13.31$  at  $E = 0$  to two sharp,  $\delta$ -function like peaks at  $\delta^{-1} = 8.17$  and  $12.9$  for  $E = -0.9999B_d$ , which are the critical values for the occurrence of the three-body bound states.

## B. Atom-dimer observables with Efimov effect

In the presence of the Efimov effect, the observables do not only depend on the mass ratio and the energy but they also depend log-periodically on the scattering length. From now on, we focus on the case of fermions with  $L = 1$ . We omit the additional subscript 1 indicating the P-wave channel for notational simplicity. We find the energy-dependent atom-dimer

scattering length for  $\delta^{-1} > 13.61$  calculated with Eq. (14) to be very well approximated by the formula

$$\tilde{a}_{AD}(\delta, k, a) \equiv \frac{-1}{k^3 \cot \delta_{AD}(\delta, k, a)} = \left\{ c_1(\delta, k) + c_2(\delta, k) \cot[s_1 \log(a/a_*) + i\eta_*] \right\} a^3. \quad (24)$$

We show  $c_{1/2}(\delta, k)$  in Fig. 5 for the mass ratios  $\delta = 0.03, 0.04,$  and  $0.06$  as functions of the momentum in units of the breakup momentum  $k_D$  from  $0.001 k_D$  up to the dimer breakup threshold. Interestingly, for all considered mass ratios,  $c_1(\delta, k) = -8.7 \pm 0.2$  for  $k \rightarrow 0$ . The coefficient  $c_2(\delta, k)$  also approaches constant values in this limit but this limit depends on the mass ratio. The smaller  $\delta$ , the larger this approached value.

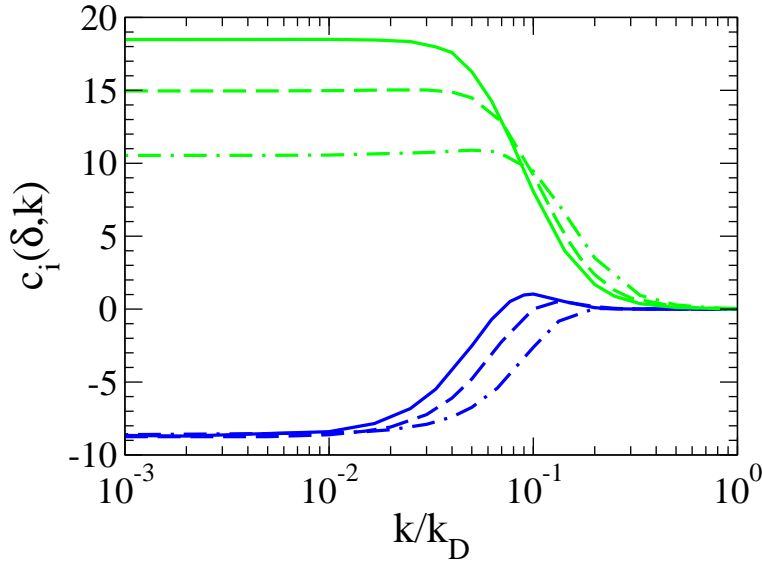


FIG. 5. Coefficients  $c_1(\delta, k)$  (dark/blue) and  $c_2(\delta, k)$  (light/green) as a function of  $k/k_D$  for mass ratios  $\delta = 0.03, 0.04,$  and  $0.06$  indicated by the solid, dashed, and dash-dotted lines, respectively.

At the dimer breakup threshold, we find

$$c_2(\delta, k_D) \approx k_D^{-3} \quad \text{and} \quad c_1(\delta, k_D) \approx 0 \quad (25)$$

to be very good approximations for  $\delta \lesssim 0.06$ . This behavior is similar to the case of spinless bosons [23]. From Eq. (17), we can deduce the atom-dimer scattering phase shift  $\delta_{AD}$  at  $E = 0$ . For  $\exp(2\pi s_1) \gg \exp(\pm 2\eta_*)$ , the expression simplifies to

$$\delta_{AD} = \sigma_1 + s_1 \ln(a/a_{0*}) + i\eta_*, \quad (26)$$

and the constraints (25) follow from Eq. (24). Since  $s_1$  approaches 0 as  $\delta \rightarrow \delta_{c,1} = 0.07349$  from below, this approximation is invalid at larger mass ratios. In this case, we find that  $c_1(\delta, k_D)$  tends to slightly larger and  $c_2(\delta, k_D)$  to slightly smaller values.

The elastic and inelastic atom-dimer scattering cross sections show the typical log-periodic dependence on the scattering length. For general momenta, they can be approximated with Eqs. (13)–(16, 24) and the appropriate coefficients from Fig. 5. At  $E = 0$ , we can compare our numerical calculation to the analytical formulae in Eqs. (18) and (19). For  $\sigma_{AD}^{(\text{inel})}(k_D)$

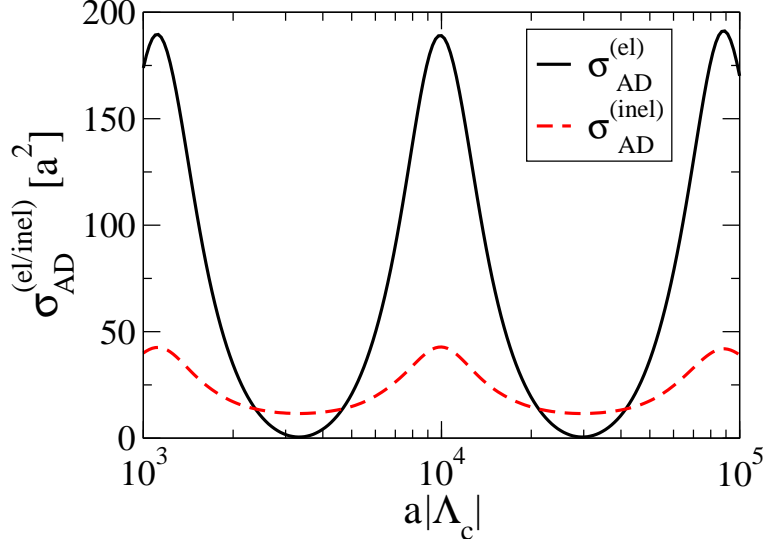


FIG. 6. Elastic (solid line) and inelastic (dashed line) atom-dimer scattering cross sections in units of  $a^2$  for  $\delta = 0.04$ ,  $\eta_* = 0.1$ , and  $E = -0.99B_d$  versus  $a|\Lambda_c|$ .

which shows only a weak dependence on  $a$ , we find generally good agreement. For the elastic cross section  $\sigma_{AD}^{(el)}(k_D)$ , we find very good agreement in the region  $\delta \lesssim 0.06$ . For larger  $\delta$ , the numerical calculation becomes difficult because of the large scaling factor.

As an example, we show the elastic and inelastic cross sections for  $\delta = 0.04$ ,  $\eta_* = 0.1$ , and  $E = -0.99B_d$  in Fig. 6. This mass ratio  $\delta$  roughly corresponds to the mixtures  ${}^7\text{Li}$ - ${}^{171/173}\text{Yb}$ . The cross sections show the typical log-periodic dependence on the scattering length. The values of the maximal and minimal cross section depend strongly on the energy and vary over several orders of magnitude. To demonstrate this dependence, we show the maximal and minimal values of  $\sigma_{AD}^{(el)}$  as a function of the center-of-mass momentum  $k/k_D$  for  $\delta = 0.03, 0.06$  and  $\eta_* = 0.2$  in Fig. 7.

The atom-dimer relaxation rate  $\beta$  which can be measured in cold atom experiments is determined by the inelastic cross section via Eq. (21). In the case of P-waves,  $\beta$  vanishes at the atom-dimer threshold  $E = -B_d$ . In Fig. 8, we show  $\beta$  for  $\delta = 0.04$  and  $0.06$ ,  $\eta_* = 0.1$ , above threshold for  $E = -0.9999B_d, -0.9984B_d, -0.96B_d$ , and  $0$ . We also give the positions of the peak in  $\beta$  for varying energy. The relaxation rate  $\beta$  shows a strong energy dependence as well. Starting from being zero at the atom-dimer threshold, it develops resonant log-periodic structures for larger energies which become less pronounced as the dimer breakup threshold is approached. The peak position is also strongly energy-dependent and varies by a factor of four for  $\delta = 0.04$  and by a factor of three for  $\delta = 0.06$ . For other mass ratios the qualitative behavior is very similar.

## VI. SUMMARY AND OUTLOOK

In this paper, we have investigated the Efimov effect for heteronuclear systems of two identical particles and a third distinguishable particle in higher partial waves. The unlike particles were assumed to have resonant S-wave interactions while the interaction between

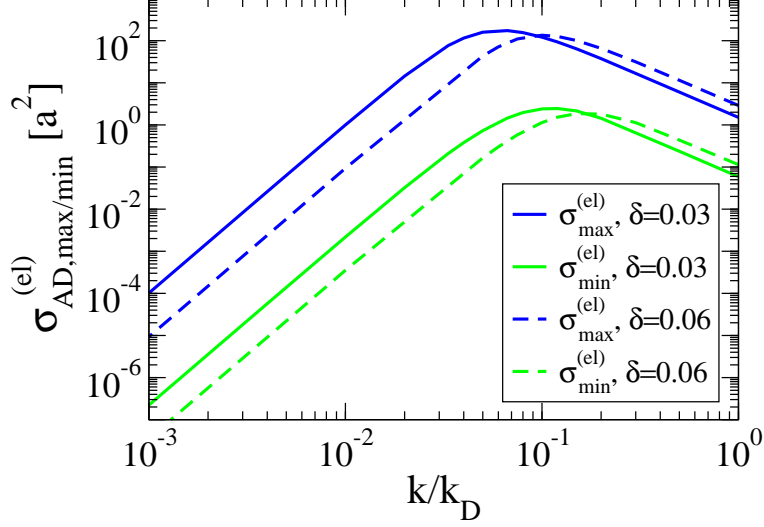


FIG. 7. Maximal and minimal values of  $\sigma_{AD}^{(el)}(k)$  as a function of  $k/k_D$  for  $\delta = 0.03$  (solid line),  $\delta = 0.06$  (dashed line) and  $\eta_* = 0.2$ .

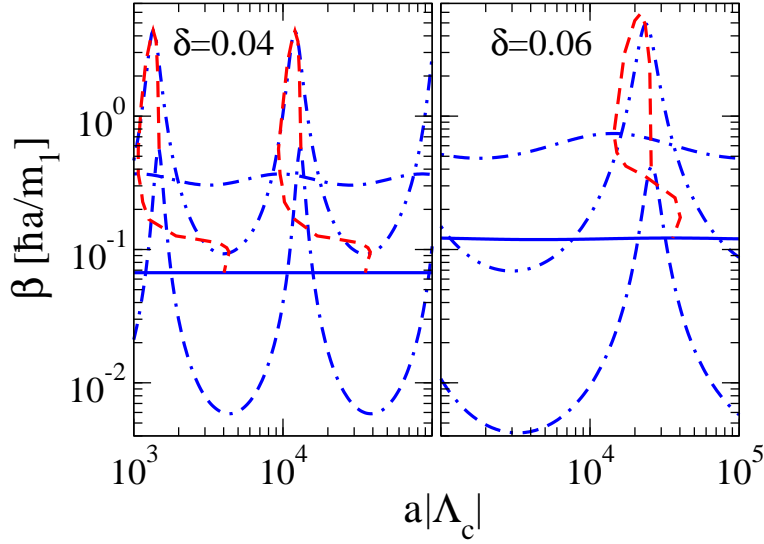


FIG. 8. Dimer relaxation rate  $\beta$  for  $\delta = 0.04$  and  $0.06$  in units of  $\hbar a/m_1$  for  $\eta_* = 0.1$  versus  $a|\Lambda_c|$ . The double-dash-dotted, dash-double-dotted, dash-dotted, and solid lines correspond to the energies  $E = -0.9999B_d$ ,  $-0.9984B_d$ ,  $-0.96B_d$ , and  $0$ , respectively. The dashed lines show how the peak position shifts with the energy.

like particles was neglected. For even (odd) angular momentum  $L$ , the two identical particles must be bosons (fermions) for the Efimov effect to occur [15]. Using an effective field theory framework, we have derived a generalized STM equation which describes the off-shell atom-dimer scattering amplitude in the total angular momentum channel  $L$ . All three-body observables can be extracted from this amplitude taken in appropriate kinematics.

We have derived a transcendental equation for the preferred scaling factor  $\exp(\pi/s_L)$

for arbitrary  $L$  as a function of the mass ratio  $\delta$ . The numerical results agree well with a previously derived equation using hypergeometric functions derived by Nielsen and coworkers [19]. For the experimentally most relevant case of the P-wave Efimov effect, we have predicted the ratio of the scattering lengths where Efimov states cross the atom-dimer and three-atom thresholds,  $a_*/|a_-|$ . This ratio is independent of the three-body parameter and can be measured in experiment. For the S-wave case, Barontini et al. [17] have measured the value  $a_*/|a_-| = 2.7$  in a K-Rb mixture. The universal prediction for this system is  $a_*/|a_-| = 0.52$ . The Efimov features in the experiment by Barontini et al. are not deeply in the universal region and thus finite range corrections are likely important for this experiment. The leading finite range correction is given by the effective range correction, but for further improvement the van der Waals tail of the interaction has to be included explicitly. Moreover, there is a finite energy shift of the atom-dimer rescattering resonance used in Ref. [17] to extract  $a_*$  that needs to be taken into account [16]. For P-waves, no experiment has been carried out to date.

The measurement of atom loss rates has played a key role for the observation of the S-wave Efimov effect in cold atoms [1] and the P-wave Efimov effect in a Bose-Fermi mixture could be detected in an analogous way. We have derived analytical expressions for the elastic and inelastic atom-dimer cross sections as well as the atom-dimer relaxation rate for arbitrary angular momentum  $L$  at the dimer breakup threshold. For energies below this threshold, we have laid out a framework to calculate these quantities numerically.

Using this framework, we have explicitly calculated the atom-dimer scattering cross sections for  $B_d < E \leq 0$  in low angular momentum channels without the Efimov effect, i.e., bosons in the P-wave and fermions in the S-Wave channel. Furthermore, we have calculated the cross section for fermions in the P-wave channel below the critical mass ratio  $\delta_{c,1}^{-1}$ . The cross section shows two peaks due to the appearance of two non-Efimov three-body bound states [29]. We have calculated the position of these peaks as a function of the collision energy  $E$ .

Focussing on the P-wave fermionic channel above the critical mass ratio, we have numerically calculated the atom-dimer cross section up to the dimer breakup threshold. The cross sections show the typical log-periodic dependence on the scattering length. The maximal and minimal cross section values depend strongly on the energy and vary over several orders of magnitude. At the atom-dimer threshold, we found good agreement with our analytical results. The atom-dimer cross section below the dimer breakup threshold can be parametrized by two universal functions  $c_1(\delta, k)$  and  $c_2(\delta, k)$ . We have calculated these functions for several mass ratios and derived simple analytical expressions for their values at the dimer breakup threshold if  $\exp(2\pi s_1) \gg \exp(\pm 2\eta_*)$  is satisfied. Finally, we have numerically calculated the atom-dimer relaxation rate  $\beta$  as a function of the three-body parameter, mass ratio and energy. As for the bosonic case [16], the position of the relaxation maxima is strongly energy dependent and not a monotonic function of energy.

In summary, our calculation provides a basis for interpreting experimental results on the Efimov effect in higher partial waves. Due to the fermionic nature of the dimers, the preparation of the required atom-dimer mixture for the P-wave case should be feasible. A few experimental groups already study heteronuclear mixtures of interest to this work, e.g. various Yb-Li mixtures in the groups of Takahashi [37] and Gupta [38]. Other groups investigate heavy species that could be mixed with Li, e.g. fermionic Sr in Grimm's group [39]. A natural extension of our work would be to calculate the three-body recombination rate for energies away from the dimer breakup threshold. This could in principle be done using

the methods of Refs. [40, 41].

## ACKNOWLEDGMENTS

We thank V. Efimov for directing our interest towards this subject. K.H. was supported by the “Studienstiftung des Deutschen Volkes” and by the Bonn-Cologne Graduate School of Physics and Astronomy. H.W.H. acknowledges support from the the Bundesministerium für Bildung und Forschung, BMBF under Contract No. 06BN9006.

- 
- [1] F. Ferlaino and R. Grimm, *Physics* **3**, 9 (2010).
  - [2] V. Efimov, *Phys. Lett. B* **33**, 563 (1970).
  - [3] B.D. Esry, C.H. Greene, and J.P. Burke, *Phys. Rev. Lett.* **83**, 1751 (1999).
  - [4] E. Braaten and H.-W. Hammer, *Phys. Rev. Lett.* **87**, 160407 (2001) [arXiv:cond-mat/0103331].
  - [5] E. Braaten and H.-W. Hammer, *Phys. Rev. A* **70**, 042706 (2004) [arXiv:cond-mat/0303249].
  - [6] T. Kraemer, M. Mark, P. Waldburger, J.G. Danzl, C. Chin, B. Engeser, A.D. Lange, K. Pilch, A. Jaakkola, H.-C. Nägerl, and R. Grimm, *Nature* **440**, 315 (2006) [arXiv:cond-mat/0512394].
  - [7] S. Knoop, F. Ferlaino, M. Mark, M. Berninger, H. Schöbel, H.-C. Nägerl, and R. Grimm, *Nature Phys.* **5**, 227 (2009) [arXiv:0807.3306 [cond-mat.other]].
  - [8] M. Zaccanti, B. Deissler, C. D’Errico, M. Fattori, M. Jona-Lasinio, S. Müller, G. Roati, M. Inguscio, and G. Modugno, *Nature Phys.* **5**, 586 (2009) [arXiv:0904.4453 [cond-mat.quant-gas]].
  - [9] N. Gross, Z. Shotan, S. Kokkelmans, and L. Khaykovich, *Phys. Rev. Lett.* **103**, 163202 (2009) [arXiv:0906.4731 [cond-mat.other]].
  - [10] S.E. Pollack, D. Dries, and R.G. Hulet, *Science* **18**, 1683 (2009) [arXiv:0911.0893 [cond-mat.quant-gas]].
  - [11] T. B. Ottenstein, T. Lompe, M. Kohnen, A. N. Wenz, and S. Jochim, *Phys. Rev. Lett.* **101**, 203202 (2008) [arXiv:0806.0587 [cond-mat.other]].
  - [12] J.H. Huckans, J.R. Williams, E.L. Hazlett, R.W. Stites, and K.M. O’Hara, *Phys. Rev. Lett.* **102**, 165302 (2009) [arXiv:0810.3288 [physics.atom-ph]].
  - [13] T. Lompe, T.B. Ottenstein, F. Serwane, A.N. Wenz, G. Zürn, and S. Jochim, *Science* **330**, 940 (2010) [arXiv:1006.2241 [cond-mat.quant-gas]].
  - [14] S. Nakajima, M. Horikoshi, T. Mukaiyama, P. Naidon, and M. Ueda, *Phys. Rev. Lett.* **106**, 143201 (2011) [arXiv:1010.1954 [cond-mat.quant-gas]].
  - [15] V. Efimov, *Nucl. Phys. A* **210**, 157 (1973).
  - [16] K. Helfrich, H.-W. Hammer, and D.S. Petrov, *Phys. Rev. A* **81**, 042715 (2010) [arXiv:1001.4371 [cond-mat.quant-gas]].
  - [17] G. Barontini, C. Weber, F. Rabatti, J. Catani, G. Thalhammer, M. Inguscio, and F. Minardi, *Phys. Rev. Lett.* **103**, 043201 (2009) [arXiv:0901.4584 [cond-mat.other]].
  - [18] B. Marcelis, S.J.J.M.F. Kokkelmans, G.V. Shlyapnikov, and D.S. Petrov, *Phys. Rev. A* **77**, 032707 (2008) [arXiv:0711.4632 [cond-mat.stat-mech]].
  - [19] E. Nielsen, D.V. Fedorov, A.S. Jensen, and E. Garrido, *Phys. Rep.* **347**, 373 (2001).

- [20] M.A. Efremov, L. Plimak, B. Berg, M.Yu. Ivanov, and W.P. Schleich, Phys. Rev. A **80**, 022714 (2009) [arXiv:0905.3974 [quant-ph]].
- [21] D.S. Petrov, Phys. Rev. A **67**, 010703(R) (2003) [arXiv:cond-mat/0209246].
- [22] O.I. Kartavtsev and A.V. Malykh, Pis'ma ZhETF **86**, 713 (2007) [arXiv:0709.4151 [physics.atom-ph]].
- [23] E. Braaten and H.-W. Hammer, Phys. Rept. **428**, 259 (2006) [arXiv:cond-mat/0410417].
- [24] G.V. Skorniakov and K.A. Ter-Martirosian, Sov. Phys. JETP **4**, 648 (1957) [J. Exptl. Theoret. Phys. (U.S.S.R.) **31**, 775 (1956)].
- [25] G.S. Danilov, Sov. Phys. JETP **13**, 349 (1961).
- [26] P.F. Bedaque, H.-W. Hammer, and U. van Kolck, Phys. Rev. Lett. **82**, 463 (1999) [arXiv:nucl-th/9809025].
- [27] H. W. Griesshammer, Nucl. Phys. **A760**, 110-138 (2005) [nucl-th/0502039].
- [28] J.P. D'Incao and B.D. Esry, Phys. Rev. A **73**, 030702(R) (2006) [arXiv:physics/0508119].
- [29] O.I. Kartavtsev and A.V. Malykh, J. Phys. B: At. Mol. Opt. Phys. **40**, 1429 (2007) [arXiv:physics/0610261].
- [30] M. Iskin, Phys. Rev. A **81**, 043634 (2010) [arXiv:1003.0106 [cond-mat.quant-gas]].
- [31] M. Iskin and C.A.R. Sá de Melo, Phys. Rev. A **77**, 013625 (2008) [arXiv:0709.4424 [cond-mat.supr-con]].
- [32] D.S. Petrov, C. Salomon, and G.V. Shlyapnikov, Phys. Rev. Lett. **93**, 090404 (2004) [arXiv:cond-mat/0309010].
- [33] D.S. Petrov, C. Salomon, and G.V. Shlyapnikov, Phys. Rev. A **71**, 012708 (2005) [arXiv:cond-mat/0407579].
- [34] J. Levinsen, T.G. Tiecke, J.T.M. Walraven, and D.S. Petrov, Phys. Rev. Lett. **103**, 153202 (2009) [arXiv:0907.5523 [cond-mat.quant-gas]].
- [35] J. Levinsen and D.S. Petrov, Eur. Phys. J. D (2011) [DOI: 10.1140/epjd/e2011-20071-x] [arXiv:1101.5979 [cond-mat.quant-gas]].
- [36] S. Endo, P. Naidon, and M. Ueda, Few-body Syst. (2011) [DOI: 10.1007/s00601-011-0229-6] [arXiv:1103.2606 [physics.atom-ph]].
- [37] H. Hara, Y. Takasu, Y. Yamaoka, J.M. Doyle, and Y. Takahashi, Phys. Rev. Lett. **106**, 205304 (2011) [arXiv:1104.4430 [physics.atom-ph]].
- [38] A.H. Hansen, A. Khramov, W.H. Dowd, A.O. Jamison, V.V. Ivanov, and S. Gupta, arXiv:1105.5751 [cond-mat.quant-gas].
- [39] M.K. Tey, S. Stellmer, R. Grimm, and F. Schreck, Phys. Rev. A **82**, 011608(R) (2010) [arXiv:1006.1131 [cond-mat.quant-gas]].
- [40] E. Braaten, H.-W. Hammer, D. Kang, and L. Platter, Phys. Rev. A **78**, 043605 (2008) [arXiv:0801.1732 [cond-mat.other]].
- [41] K. Helfrich and H.-W. Hammer, Europhys. Lett. **86**, 53003 (2009) [arXiv:0902.3410 [cond-mat.other]].